Semiconductor Optoelectronics
ISSN: 1001-5868

TRI-FORKED WITH DUAL-PORT MIMO ANTENNA FOR KU/K-BAND RADAR AND SATELLITE APPLICATIONS

Meenal Job, Amrees Pandey*, Prakhar Yadav, Ram Suchit Yadav
Department of Electronics and Communication, University of Allahabad, Prayagraj, India
Email: meenalmuduli@gmail.com, amrishpandey19@gmail.com, prakharwini@gmail.com, rsyadav_au@rediffmail.com

Abstract: It presents a compact size with 2×2 MIMO (multiple-input-multiple-output), dual Tri-forked (Trishul-shaped) antenna, enhanced gain and isolation for Ku (12-18 GHz) and K (18-27 GHz) bands of radar and satellite applications. The overall size of the proposed MIMO antenna (24×24×1.6) mm3 has been designed and simulated. The proposed MIMO antenna components are arranged parallel with identical shapes to provide a higher inter-connection element between the ports with in 50Ω characteristics impedance. The antenna covers (13.56-14.86) GHz and (16.60-18.76) GHz for Ku-band and (20.50-28.36) GHz for K-band at port-1 and 2 both respectively. The maximum/minimum peak gain of 9.06 dBi/3.26 dBi at port-1 and 2 both are observed respectively. Diversity characteristics such as envelope correlation coefficient (< 0.012), diversity gain (≤ 9.9 dB), and total active reflection coefficient (< -10 dB) determined to validate the proposed MIMO antenna's work qualities. The isolation of more than 18 dB and radiation efficiency of more than 85 % indicates that the proposed structure is suitable for using a dual-port MIMO antenna.
Index Terms- MIMO, Ku/K-band, radiation pattern, isolation, ECC, DG, TARC

1. Introduction

The prompt requirement for multiple-input multiple-output (MIMO) technology with better reliability and advanced data rates has augmented the curiosity to achieve the demand for advanced data rates for existing and progressive wireless systems [1-4]. Mutual coupling and space among the elements are always inversely proportional to each other [5-7]. Alternatively, one of the tasks of multiple and advanced wireless systems is the model of dual/triple/quad/multi-band antennas to cover the numerous assigned frequency bands for several reformed wireless applications with an acceptable recital in the entire operating bands [8-11]. The application of dual-band antennas with wide impedance bandwidth eliminates the tradition of precise multiple antennas and therefore creates the affected apparatus smaller, livelier, and inexpensive by dipping, overcoming the limitations of the previous antenna systems [12-15].

Furthermore, the multiplexing gain is important for MIMO systems; the MIMO antenna is suitable for improving data rate transmission [16-17]. Experimenters are endeavoring to structure a simple antenna to prepare high mutual coupling between ports. A very compact size

MIMO antenna anyhow degrades the accomplishment of antenna ports [18-21]. A lot of techniques have been proclaimed to decrease isolation in MIMO antenna system such as rector, meta-surface, diversity technique, and neutralized line. The distance between the radiating elements forms the MIMO structure; therefore, the enhanced role of MIMO antenna performance is based on the spacing between the elements [22]. Anyhow, the possible space is unsuitable for realistic portable devices. In this way, many techniques have been adopted to lower the isolation between MIMO elements [23-24]. Numerous MIMO antenna structures have been recently explained in the literature for Ku and K bands of radar and satellite applications [25-26]. UWB and low isolation of two port MIMO antenna for wireless communication have been reported. A comprehensive review of broadband, multiband, & UWB antennas as well as the materials and geometry numerical tools for wireless communication is reported [27]. ECC is also assessed in to assure MIMO performance.

In this paper, the goal of implementing and achieving a modest and innovative MIMO antenna, the novelty of the proposed MIMO Antenna has a lesser size (24×24×1.6 mm3) with highly isolated (between the ports), enhanced gain and better TARC as compared to reference Antenna's (cited in table 2). As compared to references, the proposed work is different because two identical shapes are arranged parallel to maximize inter-element isolation and attachment of the stub are maximize the gain.

2. Design Structure and Development of the Proposed MIMO Antenna

The dimensional structure (24×24×1.6 mm3) of the proposed antenna (step-4) has a green color (upper-view) of radiating elements and orange color (lower-view) of the ground plane dual port MIMO antenna which is fed by a 50Ω microstrip feed line (Figure 1). The proposed double are tri-forked (trishul-shaped) MIMO antenna is simulated on FR4 epoxy substrate (εr=4.4, tan δ=0.02, and thickness of 1.6 mm). The systematic growth of step-1 to step-4 is displayed in Figure 2. Antenna-1 (step-1) is achieved by introducing two identical structures with deformed are simple rectangular shaped radiating elements (10×12 mm2) (cf. Figure 2). Step-2 (Antenna-2) is obtained with the help of antenna-1 which has etched parallel rectangular slots (8×2 mm2) in radiating elements (cf. Figure 2). Step-3 (Antenna-3) is achieved by introducing Antenna-2, which has etched parallel rectangular slots (4×6 mm2) at middleware portion of the radiating elements (cf. Figure 2). The proposed antenna or step-4 (Antenna-4) is obtained from Antenna-3 which has attachment one parallel stub (11×2 mm2) in middleware portion of the radiation elements (cf. Figure 1 and 2), which have maximize the gain and bandwidth.

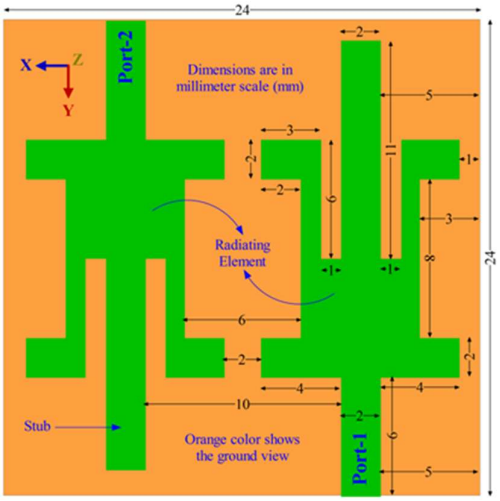

Fig. 1 Radiating-elements (green-color) and ground plane (orange-color) layout of the proposed antenna

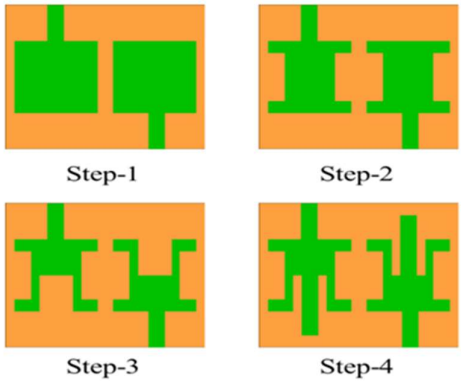

Fig. 2 Step-wise systematic development of the radiating elements (green-color) and ground plane (orange-color) layout of the antennas (step-1 to step-4)

The ground geometry of these entire antennas (step-1 to step-4) is the same, mutually coupled at ports-1 and 2. Two identical designs are deformed with tri-forked (trishul-shaped) by keeping them apart from each other at an optimized distance (2 mm) of the conducting patches to create a MIMO structure of the antennas (step-1 to step-4), the proposed antenna (step-4) which has increased the mutual coupling between the ports and also enhanced the gain. Furthermore, MIMO appearances bordering on ECC (envelope correlation coefficient), inclusive DG (diversity gain), and TARC (total active reflection coefficient) are analyzed by ANSOFT HFSS version 13, as discussed later.

3. Results and Discussion

The proposed model has been simulated in expressions of return loss (in terms of S11 and S22), radiation efficiency, gain, current distribution, mutual coupling between ports (in terms of S12 and S21), envelope correlation coefficient (ECC), radiation pattern, diversity gain (DG) and total active reflection coefficient (TARC). The proposed model is simulated by using ANSOFT High-Frequency Structure Simulator (HFSS) version 13 software.

The Table-1, represent the data in the expression of the operating band (in GHz) with bandwidth (GHz), isolation (dB), resonant frequency (GHz), return loss (dB), and peak gain (dBi) of antennas (step-1 to step-4) at port-1 and 2 are reported. The simulated analysis of step-1 to 4 in terms of |S11|, |S22|, |S12|, and |S21| are represented in the Figure 3 (a-c). The figure 3 (d) displayed the scattering parameter of the proposed antenna (step-4), and figure 3 (e) represent the gain parameter of the entire antennas (step-1 to 4).

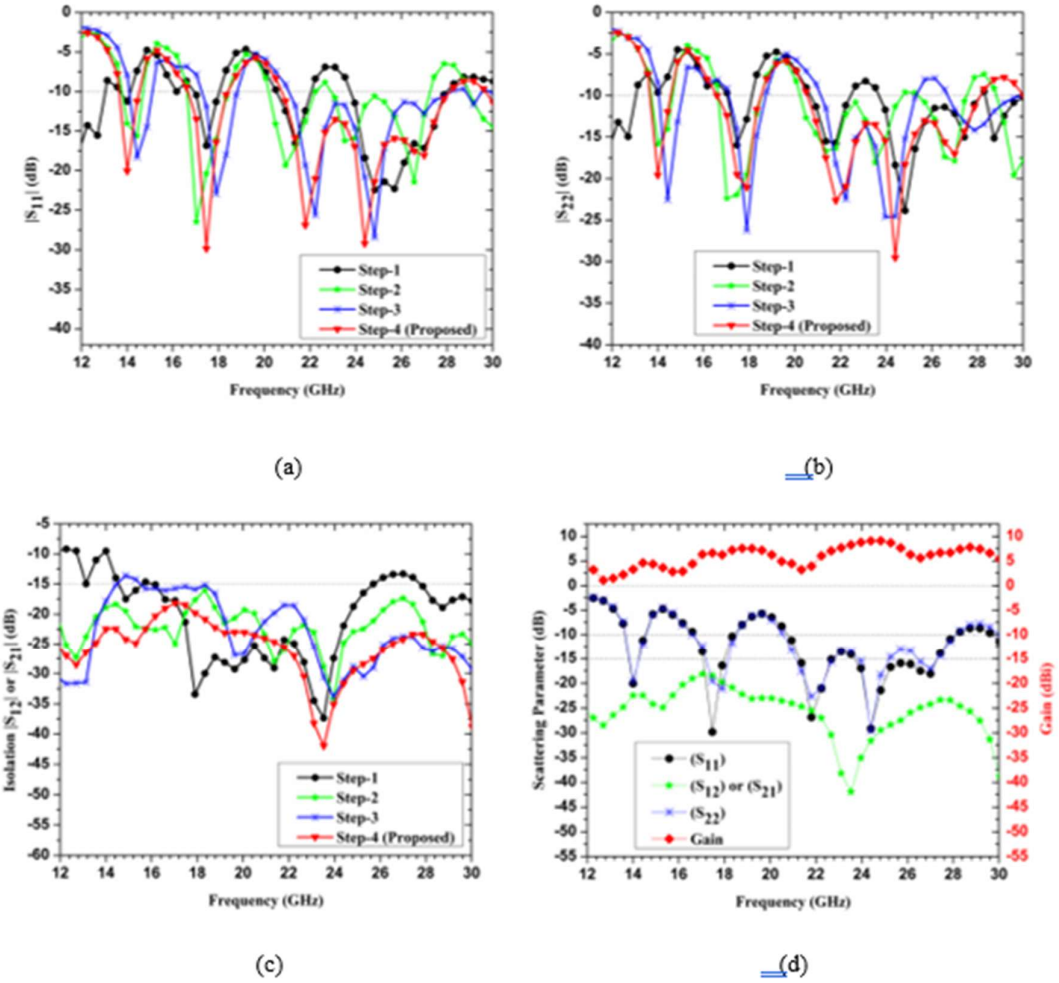

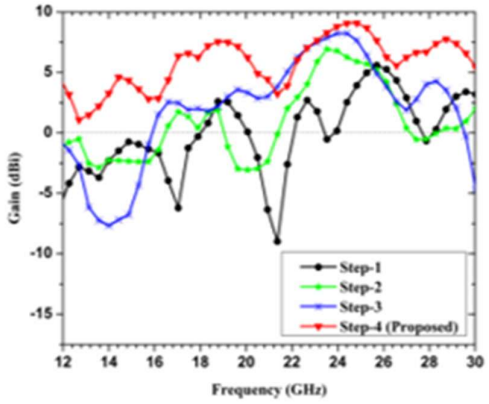

(e)

Fig. 3 Simulated analysis in terms of (a) |S11|, (b) |S22|, (c) Isolation between the ports in terms of |S12| or |S21|, (d) Scattering parameter and gain of the proposed antenna (step-4), and (e) Gain versus frequency curve of the antennas (step-1 to step-4)

However, the proposed MIMO operating bands (13.56-14.86) GHz has resonated on 14 GHz with 3.26 dBi peak gain, (16.60-18.76) GHz has resonated on 17.46 GHz with 6.59 dBi peak gain, and (20.50-28.36) GHz has resonated on 21.80 GHz, 24.40 GHz & 27 GHz with 3.89 dBi, 9.06 dBi & 6.24 dBi peak gain respectively at port-1 (cf. fig. 3 and table-1). The proposed operating bands (13.56-14.86) GHz has resonated on 14.10 GHz with 3.26 dBi peak gain, (16.60-18.76) GHz has resonated on 17.90 GHz with 6.59 dBi peak gain, and (20.50-28.36) GHz has resonated on 21.86 GHz, 24.36 GHz & 27.13 GHz with 3.89 dBi, 9.06 dBi & 6.24 dBi peak gain respectively at port-2 (cf. fig. 3 and table-1).

The proposed isolation has < 18 dB obtained, as compared to all reported antenna the proposed isolation are highly isolated, which has indicate the good agreement of radar and satellite communication. The proposed maximum/minimum peak gain 9.06/3.26 dBi at both the ports 1 & 2 respectively. The table-1 demonstrated the data of all inclusive antennas (step-1 to step-4) in terms of operating band and bandwidth (GHz), isolation (dB), reflection coefficient (dB), and peak gain (dBi).

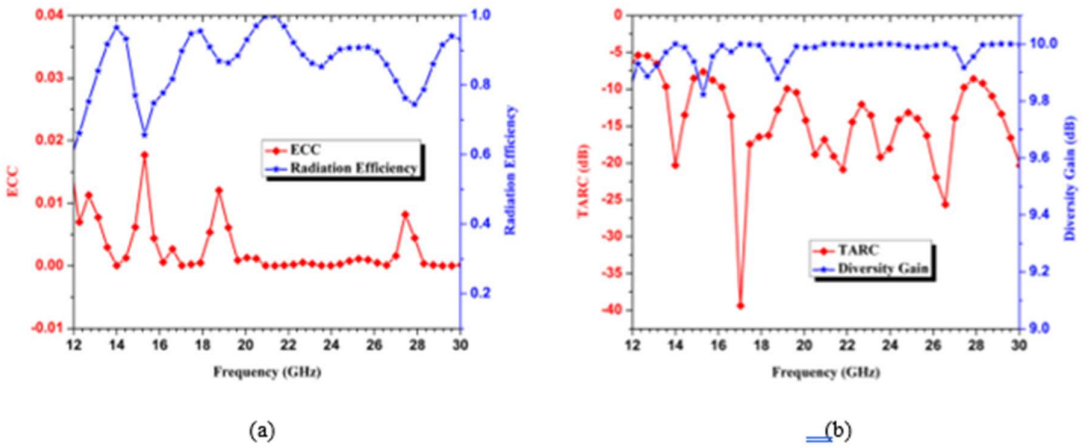

Fig. 4 Simulated analysis of the (a) ECC and Radiation Efficiency, (b) TARC and Diversity gain (DG) versus frequency curve of the proposed antenna (Step-4)

Table1: Comparative overview of the Step-1 to Step-4

Antenna	Port No.	Operating band (GHz) / Bandwidth (GHz)	Isolation (dB)	Resonant frequency (GHz)	Reflection Coefficients (dB)	Peak Gain (dBi)
Antenna-1 (Step-1)	Port-1	(13.56-14.43)/0.87	≤ 10	14.00	-11.26	-2.3
		(17.03-18.33)/1.3	≤ 17	17.46	-16.85	-1.25
		(20.50-22.23)/1.73	≤ 24	21.36	-16.51	-8.98
		(23.96-28.30)/4.34	≤ 13	24.83	-22.46	3.92
				25.70	-22.29	5.58
	Port-2	(17.03-18.33)/1.3	≤ 17	17.46	-15.98	-1.25
		(20.50-22.30)/1.8	≤ 24	21.80	-15.73	-2.60
		(23.96-28.30)/4.34	≤ 13	24.83	-23.86	3.92
				27.43	-15.01	0.96
Antenna-2 (Step-2)	Port-1	(13.56-14.86)/1.3	≤ 18	14.43	-15.62	-2.28
		(16.60-18.76)/2.16	≤ 16	17.03	-26.48	1.72
		(20.06-22.23)/2.17	≤ 19	20.93	-19.35	-2.36
		(23.10-27.43)/4.33	≤ 17	23.53	-16.23	6.92
				26.13	-16.28	4.2
	Port-2	(13.56-14.86)/1.3	≤ 18	14.00	-15.88	-2.26
		(16.60-18.76)/2.16	≤ 16	17.03	-22.40	1.72
		(20.50-24.40)/3.9	≤ 19	23.53	-18.08	6.92
		(25.70-27.43)/1.73	≤ 17	27.00	-17.88	0.38
Antenna-3 (Step-3)	Port-1	(14-15.30)/1.3	≤ 13	14.43	-18.30	-7.19
		(17.46-19.20)/1.74	≤ 15	17.9	-22.92	2.00
		(20.93-27.86)/6.93	≤ 18	22.23	-25.61	6.24
				24.83	-28.43	7.65
	Port-2	(14-15.30)/1.3	≤ 13	14.43	-18.30	-7.19
		(17.03-18.76)/1.73	≤ 15	17.90	-22.92	2.00
		(20.93-25.26)/4.33	≤ 18	23.96	-24.59	8.21
		(26.56-29.60)/3.04	≤ 18	27.86	-14.19	4.01
Antenna-4 (Step-4)	Port-1	(13.56-14.86)/1.3	≤ 22	14.00	-20.06	3.26
		(16.60-18.76)/2.16	≤ 18	17.46	-29.86	6.59
		(20.50-28.36)/7.86	≤ 23	21.80	-26.90	3.89
				24.40	-29.21	9.06
				27.00	-18.09	6.24
	Port-2	(13.56-14.86)/1.3	≤ 22	14.10	-19.60	3.26

		(16.60-18.76)/2.16	≤ 18	17.90	-21.07	6.23
		(20.50-28.36)/7.86	≤ 23	21.86	-22.66	3.89
				24.36	-29.54	9.06
				27.13	-17.03	6.24

In Table 1, we examined these antennas (step-1 to 4) and compared all these antennas; the proposed antenna (step-4) is superior in terms of bandwidth, peak gain, and isolation at both ports, i.e. port 1 and 2. In the inspection of Fig. 3 and table 1, the proposed band and gain characteristics of step-4 are almost identical at both the ports with a negligible difference between ports 1 and 2 is observed due to two symmetrical design designs being separated by a spacing (2 mm) of the radiating elements to create an MIMO structure that is placed in low-profile (24×24×1.6 mm3) of the proposed antenna (step-4).

The simulated surface current distribution of the proposed MIMO antenna is categorized at 14 GHz, 17.46 GHz, 21.80 GHz, 24.40 GHz, and 27 GHz with 62.5 A/m, 70.03 A/m, 64.5 A/m, 71.05 A/m, and 75.5 A/m respectively at port-1, and has been entirely demonstrated in Figure 5 (a-e) respectively.

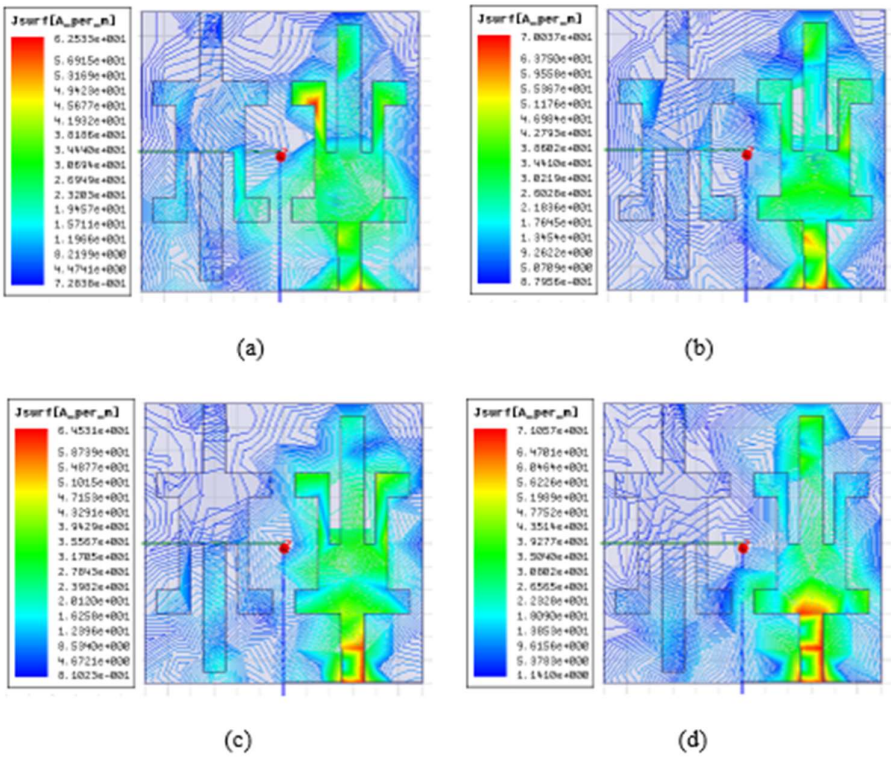

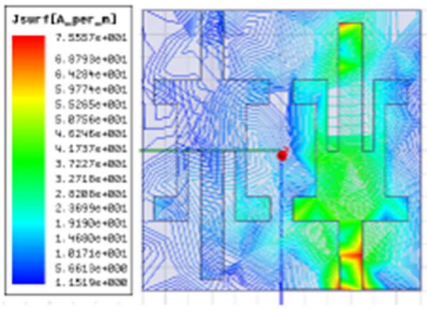

(e)

Fig. 5 Simulated surface current distributions at (a) 14 GHz, (b) 17.46 GHz, (c) 21.80 GHz, (d) 24.40 GHz and (e) 27 GHz of the proposed design (step-4) at port-1

To investigate the diversity performance of the proposed MIMO antenna, metrics like simulated ECC (envelope correlation coefficient), DG (diversity gain), and TARC (total active reflection coefficient) are reported in this section. The proposed antenna offers an ECC lower than 0.012, DG greater than 9.99 dB (near to dB), and TARC below -10 dB as a utility of frequency is displayed in Figure 4 (a, b).

Envelope correlation coefficient refers to the effect of one antenna on the performance of another. In other words, it assesses the influence of one unit cell on the performance of another unit cell. ECC of the antenna is calculated by using equation (1) to demonstrate how variation of the proposed antenna is in the acceptable limit (< 0.5) which conforms to the minimum isolation effect between antenna ports in this communication [16].

$$ECC = \frac{|S_{11}^{*}S_{12}+S_{21}^{*}S_{22}|}{(1-|S_{11}|^2-|S_{21}|^2)(1-|S_{22}|^2-|S_{12}|^2)} \quad (1)$$

$$\text{Diversity Gain} = 10 \times \sqrt{1-(ECC)^2} \quad (2)$$

Furthermore, the diversity gain is the process of the proposed antenna leads to the highest signal from a set of N signal, without increasing the input power level; the DG option enhances the signal-to-noise ratio. The following equation (2) is used to calculate the DG [18]. The figure 4 (b) represent the value of diversity gain.

The TARC (total active reflection coefficient) is one of the key factors of the MIMO antenna. It is calculated by using equation (3), the sum of the ratio of square root of total reflected power to the square root of total incident power. Thus, the proposed TARC value is less than -10 dB for the entire band (cf. Figure 4(b)). Figure 4(a) portrays the simulated radiation efficiency plots of proposed MIMO antenna more than 85% (simulated) for the entire resonating bands.

$$TARC = \frac{\sqrt{(S_{11}+S_{12})^2+(S_{22}+S_{21})^2}}{\sqrt{2}} \quad (3)$$

Figure 6 illustrates the proposed MIMO antenna is simulated Co/Cross polarization far-field

radiation patterns in both the E-plane & H-plane, when the elevation axis corresponds to the polar axis (Phi = 0o) for the antenna's coordinate system. The simulated far-field radiation pattern is presented at 14 GHz, 17.46 GHz, 21.80 GHz, 24.40 GHz, and 27 GHz, as an exhibition in figure 6 (a) to (e), respectively, at port-1. The proposed antenna is intended for entire resonating frequencies. As demonstrated, it is suitable for omnidirectional broad radiation pattern characteristics. The omnidirectional radiation patterns are operational for vehicular applications along with radar and satellite communications.

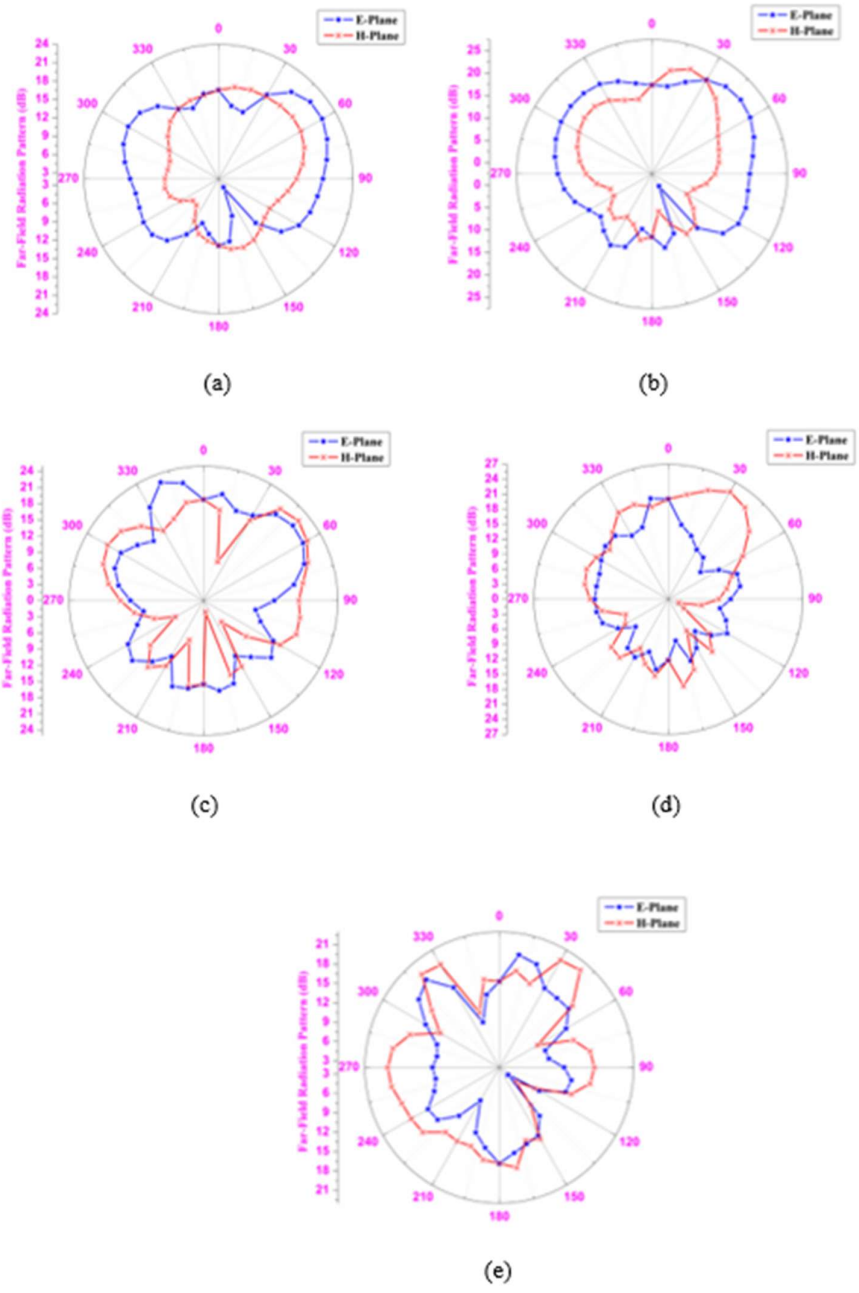

Fig. 6 Far-Field Radiation Pattern in E and H-plane for (a) 14 GHz, (b) 17.46 GHz, (c) 21.80 GHz, (d) 24.40 GHz and (e) 27 GHz of the proposed design (step-4) at port-1

4. Comparative Analysis with Modern Literature

The comparative analysis of proposed MIMO antenna with other relative MIMO antennas is mentioned in Table 2 with reference to the size of antenna, number of ports, operating bandwidth, peak gain, isolation, ECC, DG, and TARC.

Table 2: A comparative overview of the proposed MIMO antenna (step-4) with reported antenna

Ref.	Size of Antenna (mm^3)	Number of Element	Operating Band/ BW (GHz)	Peak gain (dBi)	ECC	DG (dB)	Isolation (dB)	TARC (dB)	RE (%)
[21]	42×85×0.58	2	(27-32)/5	7.9	NR	NR	-17.1	NR	70
[22]	48×21×0.13	2	(29.5-31.5)/2	7.1	0.002	9.9	-26	NR	NR
[23]	30×30×0.0009	4	(27.5-29.5)/2	5.8	0.03	10	-26	NR	80
[24]	55×50×1.6	2	(15.31-20.02)/4.7 (25.6-35.21)/9.6	7.5	0.005	9.9	-20	< 0	NR
[25]	30×52×1.6	2	(2.0-3.6)/1.6 (6.6-7.9)/1.3 (9.6-12.7)/3.1 (11-15.6)/4.6	5 3 4.2 6.6	0.024	9.9	-20	< -9.96	NR
[26]	30×30×1.6	2	(24.95-31.31)/6.36	8.2	0.0012	9.9	-15	NR	70
[27]	32×20×0.8	2	(3.3-7.8/4.5 (8.0-12.0)/4	3	0.05	9.8	-20	< 10	69
Proposed	24×24×1.6	2	(13.56-14.86)/1.3 (16.60-18.76)/2.16 (20.50-28.36)/7.86	3.26 6.59 9.06	0.012	9.9	-22 -18 -23	< -10	85

Abbreviations: ECC = Envelope Correlation Coefficient, DG = Diversity Gain, NR = Not Reported, TARC = Total Active Reflection Coefficient, BW = Bandwidth, RE = Radiation Efficiency

The proposed design is compact (in size) and much superior performance in standings of operating band, bandwidth, gain, ECC, isolation, DG and TARC than other reported band MIMO antennas in the literature [21-27]. Still, the proposed antenna exhibits a higher peak gain, enhanced envelope correlation coefficient (ECC), acceptable diversity gain (DG), well isolation and total active reflection coefficient (TARC) as related to the described antennas in reference [21-27].

5. Conclusion

The purpose of this communication is too designed tri-forked a compact (24×24×1.6 mm3), dual-port MIMO antenna with enhanced gain and isolation for the Ku and K bands of radar and satellite applications. The two identical shapes are arranged parallel to maximize inter-element isolation. The proposed design is simulated on FR-4 epoxy substrate ($\varepsilon r = 4.4$, $\tan \delta = 0.02$ and $h = 1.6$ mm) and carried out by ANSOFT HFSS 13 electromagnetic solver, and its simulated results of the proposed antenna gain varies in the range of (3.26-9.06) dBi, which include maximum/minimum peak gain of 9.06/3.26 dBi at port-1 & 2 are both, diversity gain (DG) is in the acceptable range (very close to 10 dB) between (9.99-10) dB, TARC < -10 dB,

and radiation efficiency is more than 85% is obtained during the entire operating frequency bands is observed. The operating band and gain characteristics of the proposed antenna are matched at ports 1 and 2, which conforms to good mutual coupling and admirable simulated isolation ≤ -18 dB between antenna elements (port 1 and 2) and ECC < 0.012. The Omni-directional radiation pattern of the proposed antenna is beneficial even for vehicular applications along with radar and satellite communications.

References

Rahimian, A. and F. Mehran, “RF link budget analysis in urban propagation microcell environment for mobile radio communication systems link planning," 2011 International Conference on Wireless Communications and Signal Processing (WCSP), 1-5, IEEE, November 2011.

Wang, C. X., F. Haider, X. Gao, X. H. You, Y. Yang, D. Yuan, and E. Hepsaydir, “Cellular architecture and key technologies for 5G wireless communication networks," IEEE Communications Magazine, Vol. 52, No. 2, 122-130, 2014.

Tan, C. M. and M. R. Tripathy, “A miniaturized T-shaped MIMO antenna for X-band and Ku-band applications with enhanced radiation efficiency," 2018 27th Wireless and Optical Communication Conference (WOCC), 1-5, IEEE, April 2018.

Pouyanfar, N., C. Ghobadi, J. Nourinia, K. Pedram, and M. Majidzadeh, “A compact multi-band MIMO antenna with high isolation for C and X bands using defected ground structure," Radio engineering, Vol. 27, No. 3, 686-693, 2018.

Li, Y., C. Wang, H. Yuan, N. Liu, H. Zhao, and X. Li, “A 5G MIMO antenna manufactured by 3-D printing method," IEEE Antennas and Wireless Propagation Letters, Vol. 16, 657-660, 2016.

Wang, Q., N. Mu, L. Wang, et al., “5G MIMO conformal microstrip antenna design," Wireless Comms. and Mobile Computing, 1-11, 2017.

Alhalabi, R. A. and G. M. Rebeiz, ‘High-efficiency angled-dipole antennas for millimeter-wave phased array applications," IEEE Transactions on Antennas and Propagation, Vol. 56, No. 10, 3136-3142, 2008.

Jilani, S. F. and A. Alomainy, “A multiband millimeter-wave 2-D array based on enhanced Franklin antenna for 5G wireless systems," IEEE Antennas and Wireless Propagation Letters, Vol. 16, 2983-2986, 2017.

Hussain, R., A. T. Alreshaid, S. K. Podilchak, and M. S. Sharawi, “Compact 4G MIMO antenna integrated with a 5G array for current and future mobile handsets," IET Microwaves, Antennas & Propagation, Vol. 11, No. 2, 271-279, 2017.

Wu, D., S. W. Cheung, T. I. Yuk, and X. L. Sun, “A planar MIMO antenna for mobile phones, "PIERS Proceedings, 1150{1152, Taipei, March 25-28, 2013.

OuYang, J., F. Yang, and Z. M. Wang, “Reducing mutual coupling of closely spaced microstrip MIMO antennas for WLAN application," IEEE Antennas and Wireless Propagation Letters, Vol. 10, 310-313, 2011.

Chiu, C. Y., C. H. Cheng, R. D. Murch, and C. R. Rowell, “Reduction of mutual coupling between closely-packed antenna elements," IEEE Transactions on Antennas and Propagation, Vol. 55, No. 6, 1732-1738, 2007.

Chilukuri, S., K. Dahal, and A. Lokam, “Multi-port pattern diversity antenna for K and

Ka-band application," Advanced Electromagnetics, Vol. 7, No. 2, 5-9, 2018.

Murali Krishna, C., M. Sai Prapoorna, K. Taruni Sesha Sai, and M. Sai Teja, "Super wideband MIMO antenna for advanced wireless communication," Advances in Electrical and Computer Technologies, 509-519, Springer, Singapore, 2021.

Park, J. S., J. B. Ko, H. K. Kwon, B. S. Kang, B. Park, and D. Kim, "A tilted combined beam antenna for 5G communications using a 28-GHz band," IEEE Antennas and Wireless Propagation Letters, Vol. 15, 1685-1688, 2016.

Urimubenshi, F., D. B. Konditi, J. de Dieu Iyakaremye, P. M. Mpele, and A. Munyaneza, "A novel approach for low mutual coupling and ultra-compact two port MIMO antenna development for UWB wireless application," Heliyon, Vol. 8, No. 3, e09057, 2022.

Cicchetti, R., E. Miozzi, and O. Testa, "Wideband and UWB antennas for wireless applications: A comprehensive review," International Journal of Antennas and Propagation, 2017.

Dwivedi, A. K., A. Sharma, A. K. Singh, and V. Singh, "Circularly polarized quad-port MIMO dielectric resonator antenna with beam tilting feature for vehicular communication," IETE Technical Review, 1-13, 2020.

Dwivedi, A. K., A. Sharma, A. K. Singh, and V. Singh, "Meta-material inspired dielectric resonator MIMO antenna for isolation enhancement and linear to circular polarization of waves," Measurement, Vol. 182, 109-681, 2021.

Addepalli, T. and V. R. Anitha, "Compact two-port MIMO antenna with high isolation using parasitic reectors for UWB, X and Ku band applications," Progress In Electromagnetics Research C, Vol. 102, 63-77, 2020.

Sehrai, D. A., M. Abdullah, A. Altaf, S. H. Kiani, F. Muhammad, M. Tufail, and S. Rahman, "A novel high gain wideband MIMO antenna for 5G millimeter wave applications," Electronics, Vol. 9, No. 6, 1031, 2020.

Rahman, S., X. C. Ren, A. Altaf, M. Irfan, M. Abdullah, F. Muhammad, and F. S. AlKahtani, "Nature inspired MIMO antenna system for future mm-Wave technologies," Micromachines, Vol. 11, No. 12, 1083, 2020.

Rappaport, T. S., Y. Xing, G. R. MacCartney, A. F. Molisch, E. Mellios, and J. Zhang, "Overview of millimeter wave communications for fifth-generation (5G) wireless networks with a focus on propagation models," IEEE Transactions on Antennas and Propagation, Vol. 65, No. 12, 6213-6230, 2017.

Sharawi, M. S., S. K. Podilchak, M. T. Hussain, and Y. M. Antar, "Dielectric resonator based MIMO antenna system enabling millimetre-wave mobile devices," IET Microwaves, Antennas & Propagation, Vol. 11, No. 2, 287-293, 2017.

Saxena, G., P. Jain, and Y. K. Awasthi, "High diversity gain super-wideband single band-notch MIMO antenna for multiple wireless applications," IET Microwaves, Antennas & Propagation, Vol. 14, No. 1, 109-119, 2020.

Bhatia, S. S. and N. Sharma, "Modified spokes wheel shaped MIMO antenna system for multiband and future 5G applications: Design and measurement," Progress In Electromagnetics Research C, Vol. 117, 261-276, 2021.

Pandey, A., A. K. Singh, S. Singh, and R. Singh, "A compact Ultra-Wideband (UWB) MIMO antenna for K and Ka band applications," IOT with Smart Systems, 117-126, Springer, Singapore, 2022.